

Demonstration of KV-Class β -Ga₂O₃ Trench Junction Barrier Schottky Diodes with Space-Modulated Junction Termination Extension

Advait Gilankar^{1,a)}, Julian Gervassi-Saga¹, Martha R. McCartney², Nabasindhu Das¹, David Malcolm McComas¹, David J. Smith² and Nidhin Kurian Kalarickal¹

¹School of Electrical, Computer and Energy Engineering, Arizona State University, Tempe, AZ 85281

²Department of Physics, Arizona State University, Tempe, AZ 85287

a) Electronic mail: agilanka@asu.edu

In this work, we report on the design and fabrication of p-NiO/Ga₂O₃ trench junction barrier schottky diodes (JBSD) integrated with space-modulated junction termination extension (SM-JTE) and compare the performance with planar Ni/Ga₂O₃ schottky diodes (SBDs) and p-NiO/Ga₂O₃ heterojunction diodes (HJDs). The JBSDs achieved breakdown voltages exceeding 1.8 kV along with low leakage currents ($<10^{-2}$ A/cm²), while displaying low turn on voltage (V_{ON}) of ~ 1 V, which is similar to that of planar Ni/Ga₂O₃ SBDs. The fabricated devices showed excellent forward characteristics with low differential on-resistance ($R_{on,sp}$) ranging from 4-10.5 m Ω -cm², for fin width between 0.6-1.25 microns. Best performing device with fin width of 0.85 μ m showed a unipolar figure of merit (FOM) of ~ 0.7 GW/cm². This work showcases the benefits of trench JBS design along with SM-JTE edge-termination for efficient high-performance kilovolt-class β -Ga₂O₃ diodes.

I. INTRODUCTION

The growing demand for high performance, energy efficient power devices capable of operating at higher power densities and frequencies, as well as in harsh environments have compelled researchers to investigate semiconductor technologies beyond conventional materials such as Si, SiC and GaN.¹⁻³ In this context, ultra-wide bandgap semiconductors having a bandgap (E_g) larger than 3.4eV have attracted considerable attention over the past decade. Among UWBGs, β -Ga₂O₃ ($E_g=4.8\text{eV}$) has emerged as a highly promising candidate for applications in high-power electronics, owing to its high theoretical breakdown field (8 MV/cm) and wider range of n-type doping capability.⁴⁻⁶ Additionally, the availability of large-area single-crystal substrates grown using bulk crystal growth techniques have enabled high quality homoepitaxy using various techniques such as Halide Vapor Phase Epitaxy (HVPE), Metal Organic Vapor Phase Epitaxy (MOVPE) and Molecular Beam Epitaxy (MBE).^{7,8} High quality drift layers with low defect densities have enabled the demonstration high-performance small and large-area ($>1\text{mm}^2$) devices with several recent reports having surpassed the unipolar figure of merit (FOM) of SiC and GaN.^{9,10}

Despite the above-mentioned advantages, β -Ga₂O₃ technology faces two key limitations: 1) the low-thermal conductivity of β -Ga₂O₃ and 2) the absence of reliable p-type doping to form p-n homojunctions.^{4,5} While a β -Ga₂O₃ homo p-n junction may be impractical for power switching due to the large turn on voltage ($\sim 4.5\text{ V}$), these junctions are essential for enabling advanced power device architectures such as junction barrier schottky diodes (JBSDs), D-MOSFETs and Trench-MOSFETs.^{11,12} In addition, these junctions are also key to realizing high performance field terminations such as guard rings and junction termination, which are critical for achieving near theoretical

breakdown performance.^{13,14} Researchers have been successful in circumventing this drawback by using p-type oxide based hetero p-n junctions (such as p-NiO/n-Ga₂O₃ heterojunction).^{15–18} In recent years, multiple groups have demonstrated p-NiO/ β -Ga₂O₃ heterojunction diodes (HJDs) utilizing edge terminations such as field plates, implant terminations, high-k dielectrics and JTEs (using p-NiO) achieving record high performance for 2-terminal devices.^{15,19–21}

The primary drawback of p-NiO/ Ga₂O₃ HJDs is high (>2V) turn-on voltage which results in higher conduction losses in the on-state.^{22,23} One way to overcome the challenge of high turn-on voltage is to fabricate junction barrier schottky diodes (JBSDs) which simultaneously offer benefits of low turn-on voltage and high reverse breakdown voltage. There have been prior reports employing the use of p-NiO on Ga₂O₃ to achieve high-performance JBSDs.^{24–26} Additionally, trench Schottky barrier diodes (SBDs) have also been demonstrated in the past achieving high breakdown voltage, due to reduced surface field (ReSURF) effect at the Schottky metal/semiconductor junction.¹⁰

In this work, we demonstrate a deep trench-junction barrier schottky diode (JSBD) which simultaneously leverages the higher breakdown field of the NiO/Ga₂O₃ junction (at the trench corner) and the RESURF effect due to the trench design (at the Schottky contact) for enhanced breakdown voltage. In addition, the JBSDs are integrated with an effective space-modulated junction termination extension (SM-JTE) as the edge termination. The fabricated JBSDs display a low turn on voltage of ~ 1 V, which is significantly lower than that of planar NiO/Ga₂O₃ HJDs fabricated on the same wafer. The diodes also achieve a high breakdown voltage between 1.8 and 2 kV, which is $\sim 2\times$

higher compared to planar NiO/Ga₂O₃ HJDs (without edge termination) and around $\sim 4\times$ higher compared to planar Ni/Ga₂O₃ SBDs (without edge termination).

II. EXPERIMENTAL AND DEVICE CHARACTERIZATION

The devices were fabricated on halide vapor phase epitaxy (HVPE) grown 10 μ m thick (001) β -Ga₂O₃ drift-layer procured from Novel Crystal Technologies (NCT), Japan, with doping concentration of $\sim 1.1 \times 10^{16} \text{ cm}^{-3}$. The doping concentration in the substrate was estimated to be $\sim 5 \times 10^{18} \text{ cm}^{-3}$. The sample underwent a standard solvent clean and HF dip for about 15 minutes, following which the alignment marks were patterned and etched into the sample using ICP-RIE dry-etch. This was followed by e-beam evaporation of Ti/Au (50/100nm) backside ohmic contacts and subsequent rapid thermal annealing (RTA) at 470°C for 1 minute in N₂ environment. A tri-layer hard mask consisting of SiO₂ (300nm), SiN_x (100nm) and Ni (100nm) was used to pattern Ga₂O₃ trenches. First the SiO₂ and SiN_x layers under the Ni were etched away using a CHF₃/O₂ RIE etch. Afterwards, the Ga₂O₃ trenches were defined using BCl₃ gas-based ICP dry-etch process with ICP and RF power of 800W and 30W, respectively. The diodes were patterned to have different fin-widths (W_f) which varied from 0.6 μ m to 1.25 μ m with an estimated trench depth of 0.85 μ m. Post dry etching of trenches, the Ni layer in the tri-layer mask was removed using HCl. A controlled dip in diluted BOE (1:10) was used to create an undercut in the SiO₂/SiN_x mask making use of the vastly different etch rates for these dielectrics in BOE. Following the dry-etch process, 150nm thick p-NiO was deposited using RF sputtering in 10% O₂/ Ar environment. NiO sputtering was carried out using an 8" NiO target at pressure of 4mT and RF power of 300W. Due to the undercut in the SiO₂/SiN_x mask, the NiO deposited on the top-side of the trenches could

be easily lifted off by performing a short dip in dilute BOE (1:10), leaving NiO only on the trench bottom and the sidewalls. The space-modulated JTE was formed by a two-step NiO deposition with 50nm and 100nm thickness. Following NiO sputtering, devices were RTP annealed in N₂ at 300°C for 300s. Finally, a thick metal stack Ni/Au (50nm/80nm) was evaporated to form the Schottky contact as well as the ohmic contact to the p-NiO. The process flow used for the fabrication of trench JBSDs and schematic showing critical steps is summarized in Fig. 1. Planar p-NiO/ Ga₂O₃ HJDs (thickness of NiO ~150nm) and Ni/Ga₂O₃ SBDs were also fabricated on the same epi-layer alongside the trench SM-JTE diodes. The cross-sectional schematic of the device after fabrication is shown in Fig. 2 (a)-(b). Post-fabrication, the devices were electrically characterized using Keysight B1500A parameter analyzer and B1505A high-voltage analyzer. Sample for TEM imaging was prepared by focused ion beam (FIB) milling using Thermo Fisher Helios 5 UX. The HR-TEM imaging of the cross-section of trench structure was performed using an image-corrected FEI Titan 80–300 operated at 300 kV. The cross-sectional TEM image of trench SM-JTE diode with fin-width of 0.6μm is shown in Fig. 2(c).

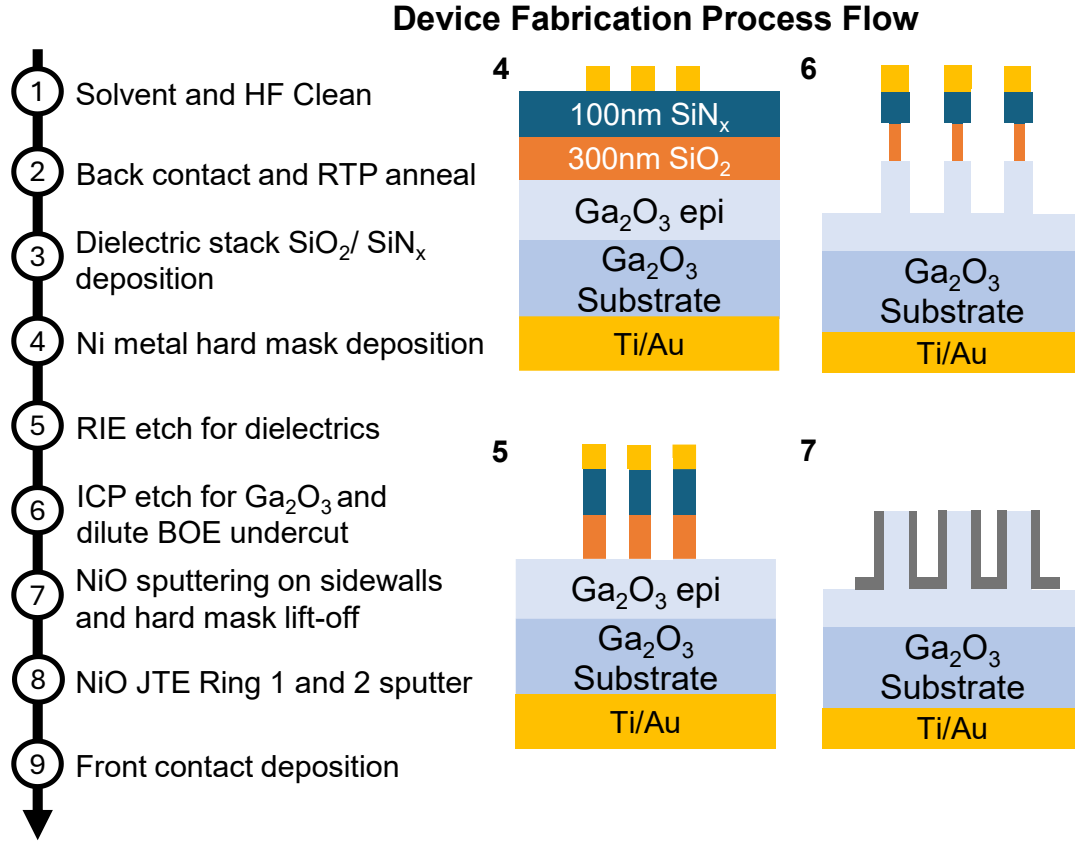


FIG. 1. Schematic of process flow used for device fabrication and schematic showing critical fabrication steps 4-7.

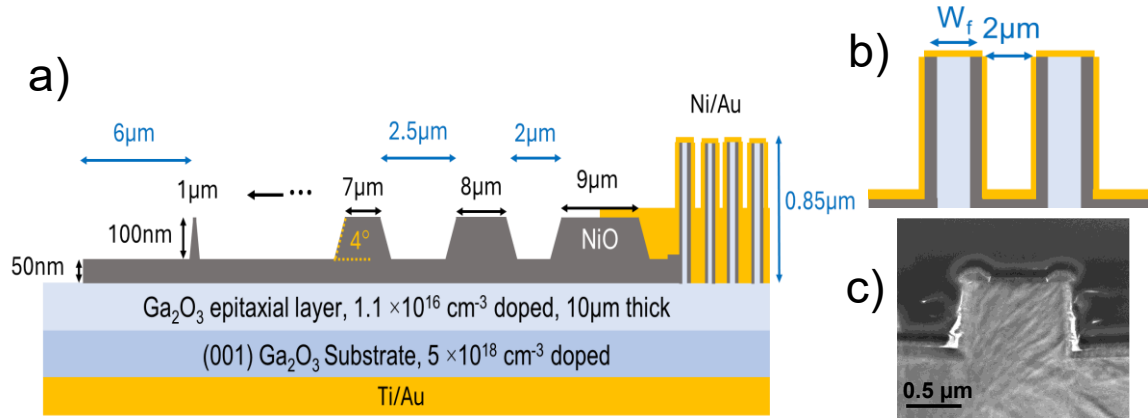


FIG. 2. Device schematic of deep trench SM-JTE JBSDs: **(a)** complete device schematic, **(b)** magnified cross-sectional schematic of the trench structure, and **(c)** Cross-sectional HR-TEM image of device with 0.6 μm fin-width.

III. RESULTS AND DISCUSSION

The donor concentration in the Ga_2O_3 epilayer is estimated using C-V measurements as shown in Fig. 4(b). The net donor concentration ($N_D - N_A$) in the drift-layer is estimated to be $\sim 1.1 \times 10^{16} \text{ cm}^{-3}$. The forward current-voltage (I-V) characteristics of diodes with different fin-widths (W_f) are shown in Fig. 3 (a) and (b). The forward currents are normalized with respect to total fin area. The specific differential on-resistance ($R_{\text{on,sp}}$) for diodes with different fin-widths is shown in Fig. 3(c). The $R_{\text{on,sp}}$ (normalized to fin-widths) varies from about $4 \text{ m}\Omega\text{-cm}^2$ ($W_f = 1.25 \mu\text{m}$) to $10.5 \text{ m}\Omega\text{-cm}^2$ ($W_f = 0.6 \mu\text{m}$).

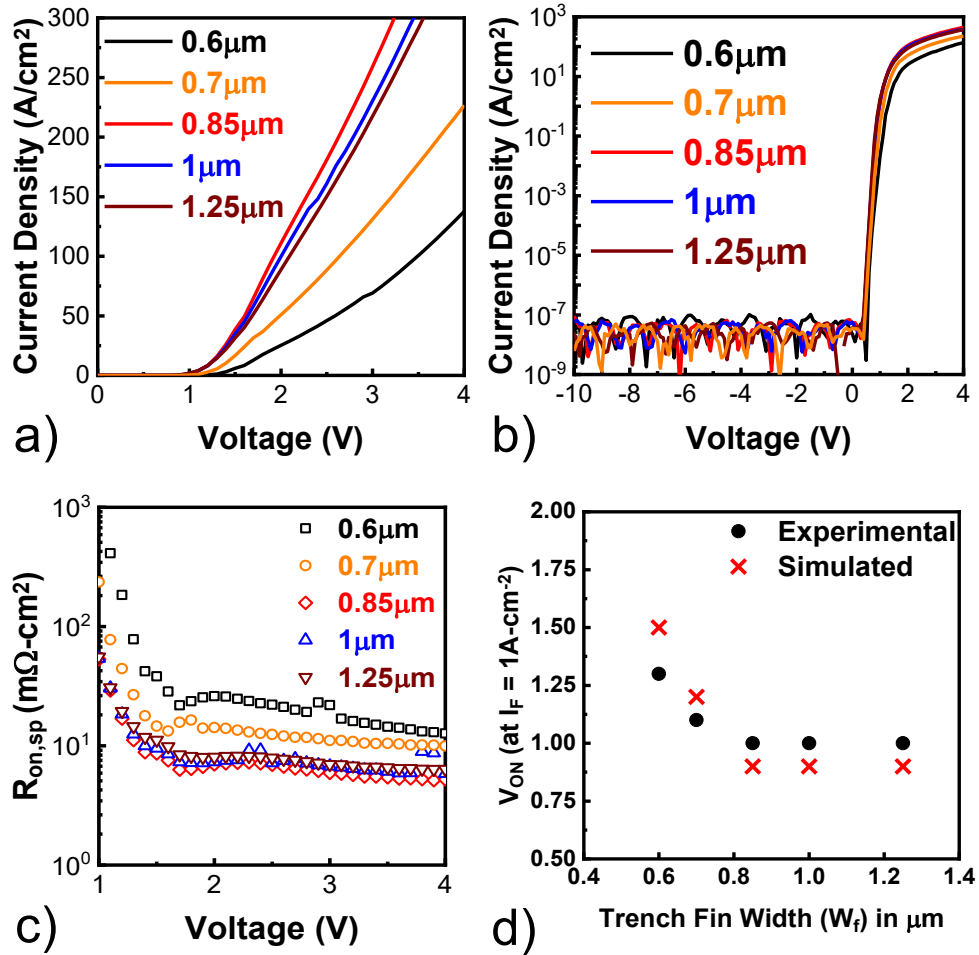


FIG. 3. Forward I-V characteristic for trench diodes with different fin-widths in **(a)** linear scale, **(b)** semi-log scale. **(c)** Plot showing differential on-resistance ($R_{on,sp}$) versus voltage for different fin-widths (The forward I-V was normalized with respect to total fin-width area). **(d)** Comparison of turn-on voltage at current density of 1A-cm^{-2} (V_{ON}) as a function of trench fin-width (W_f) extracted from simulated and experimentally measured forward I-Vs.

All the JBSDs display a low turn-on voltage between 1 and 1.3V (extracted at 1A-cm^{-2}), and the forward current density increases as the fin-width increases. In fig. 3(d), we observe that the turn-on voltage of JBSD decreases as the fin-width increases, with devices having $W_f > 0.85\text{ }\mu\text{m}$ displaying a constant V_{ON} of $\sim 1\text{ V}$. This trend is supported by TCAD simulations of the device structure under forward bias conditions. This suggest that devices with $W_f < 0.85\text{ }\mu\text{m}$ do not offer optimal performance in terms of the turn on voltage. The forward turn-on characteristics of the trench JBS diodes were also compared with planar SBDs and HJDs as shown in Fig. 4 (a). The SBDs and trench JBSDs show nearly similar forward performance in terms of both turn-on voltage and forward current density. The SBD and trench JBSD ($W_f = 0.85\mu\text{m}$) show turn-on voltage of 0.8V and 1V respectively measured at a current density of 1 A-cm^{-2} . The NiO/Ga₂O₃ HJD, however, displays a much higher turn-on voltage of around 2.5V. In addition to higher turn-on voltage, the HJD is also more resistive and shows lower forward current density recorded at same voltage compared to trench JBSDs.

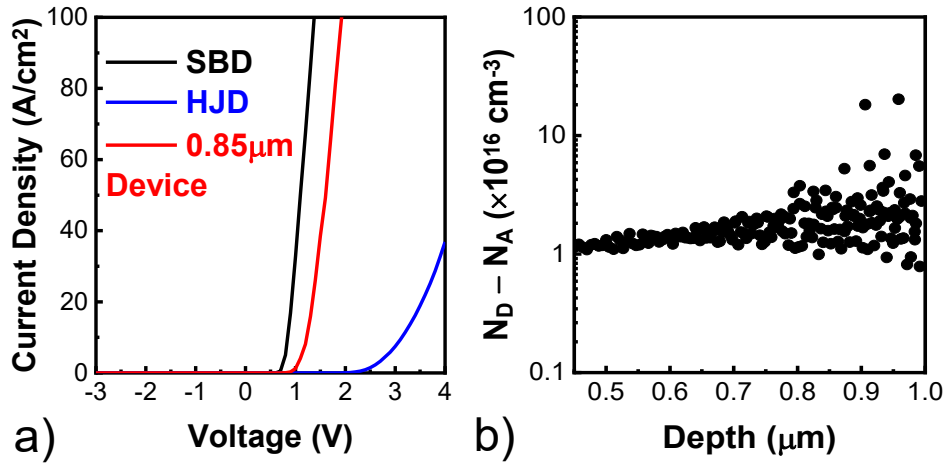


FIG. 4. **(a)** Comparison of forward I-V characteristics of Ni/Ga₂O₃ (SBD), (150nm thick NiO) NiO/Ga₂O₃ (HJD) and trench JBSD. **(b)** Net charge concentration extracted from C-V measurements is shown.

The measured reverse I-V characteristics of the devices (JBSDs, SBDs and HJDs) is shown in Fig. 5 (a). The reverse leakage current for the JBSDs is normalized to the total device area (active area + JTE area).

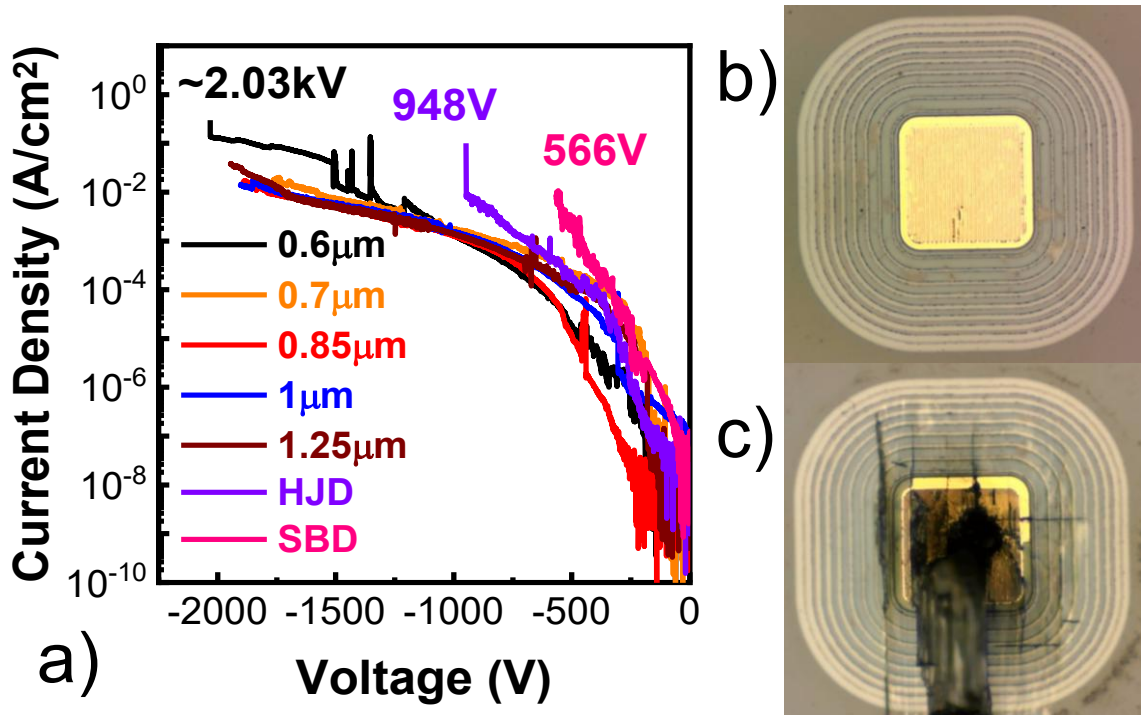


FIG. 5. **(a)** Reverse I-V characteristics for trench JBS diodes with different fin-widths, SBD, and HJD. Optical images of trench JBS diodes with fin-width of $0.6\mu\text{m}$ devices **(b)** before breakdown, and **(c)** post-breakdown.

The hard breakdown voltage of the trench JBSDs ranged from 1.8-2kV, while the planar SBDs and HJDs showed significantly lower breakdown voltages of 566V and 948V, respectively. This shows the effectiveness of the trench design and the SM-JTE compared to that of the planar devices without edge termination. The optical images of the devices pre-breakdown and post-breakdown are shown in Fig. 5 (b), (c), respectively. Most devices broke down due to high electric fields at the trench-corner or at the edge of the SM-JTE edge termination (discussed later). The trench width of the JBSDs showed no significant impact on the breakdown voltage as shown in Fig. 5 (a). This is likely due to the breakdown occurring at the trench corners where the peak field only shows a marginal increase with increasing fin width (Fig. 6 (b)) or at the edge of the SM-JTE, where the field is independent of the fin width. Furthermore, from the TEM images we observe PR residue at the trench corners (between the metal and NiO) which likely also compromised the breakdown field of the NiO/Ga₂O₃ junction at the trench corner. An optimized process would enable further enhancement of the overall junction breakdown field and the breakdown voltage of the JBSDs.

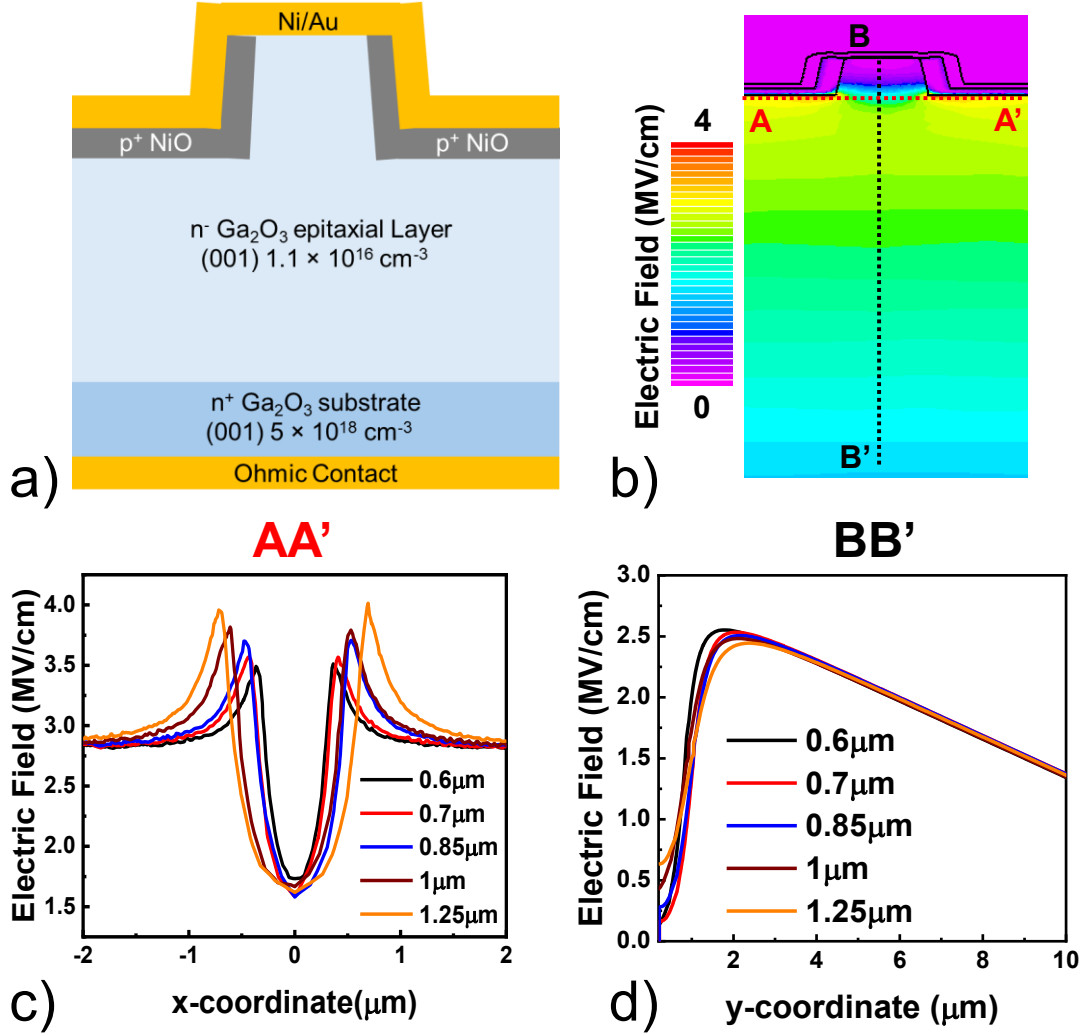


FIG. 6. TCAD silvaco simulation for trench JBSD with fin-width of $0.6 \mu\text{m}$ at 2kV reverse bias is shown. **(a)** Schematic of a single-fin from trench JBS diodes. **(b)** Electric field contours showing 2 different outlines AA' (horizontal line through Ga₂O₃ just at the NiO/Ga₂O₃ interface) and BB' (vertical line through Ga₂O₃ from top to bottom). **(c)** Plot of electric field vs x-coordinate (showing electric field distribution along AA'), and **(d)** Plot of electric field vs y-coordinate (showing electric field distribution along BB').

TCAD simulations for the trench diodes were performed using Silvaco to get additional insights into the field distribution within the device. The doping concentration in the NiO layer used is $4 \times 10^{18} \text{ cm}^{-3}$ which is estimated from C-V measurements of NiO/Ga₂O₃ diodes (fabricated on n⁺ Ga₂O₃ substrate co-loaded during NiO sputtering). TCAD

simulation results for trench JBSDs with varying fin-widths are shown in Fig. 5. The schematic of trench JBSD is shown in Fig. 6(a). The mesa angle at the fin bottom is about 83° . The electric field contour plot is shown in Fig. 6(b) and the electric field profile along cutlines AA' and BB' is shown in Fig. 6(c)-(d), respectively. At a reverse bias of 2 kV, the peak electric field at the trench corner varies between 3.5 and $4 \text{ MV}\cdot\text{cm}^{-1}$ for fin-widths (W_f) between $0.6\mu\text{m}$ and $1.25\mu\text{m}$, respectively. Due to the trench design, we are able to reduce the electric field at the metal/ Ga_2O_3 interface to $<0.6 \text{ MV}\cdot\text{cm}^{-1}$ for all fin-widths used in this work (see Fig. 6(d)). This RESURF design prevents the premature breakdown due to high electric fields at the metal/ semiconductor junction.

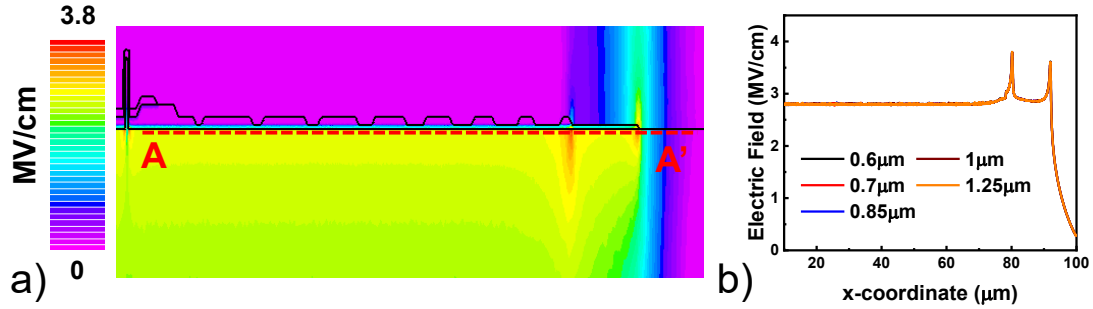


FIG. 7. TCAD silvaco simulations for trench JBSDs with SM-JTE edge termination at a reverse bias of 2kV. **(a)** Electric field contour at a reverse bias of 2 kV (horizontal line inside Ga_2O_3 at interface of $\text{NiO}/\text{Ga}_2\text{O}_3$), **(b)** Electric field along the cutline A-A' (see (b)) for devices with different fin-widths.

We also performed complete device TCAD simulations incorporating both the trench-structure and the SM-JTE edge termination as shown in Fig. 7. The electric field distribution along the horizontal cutline AA' is shown in Fig. 7(b) where we see 2 peak electric fields, one at the edge of JTE rings, and the other one at the edge of thin JTE layer, which is approximately $3.8 \text{ MV}\cdot\text{cm}^{-1}$ (note that the peak electric field occurring at fin bottom is shown in Fig. 6).

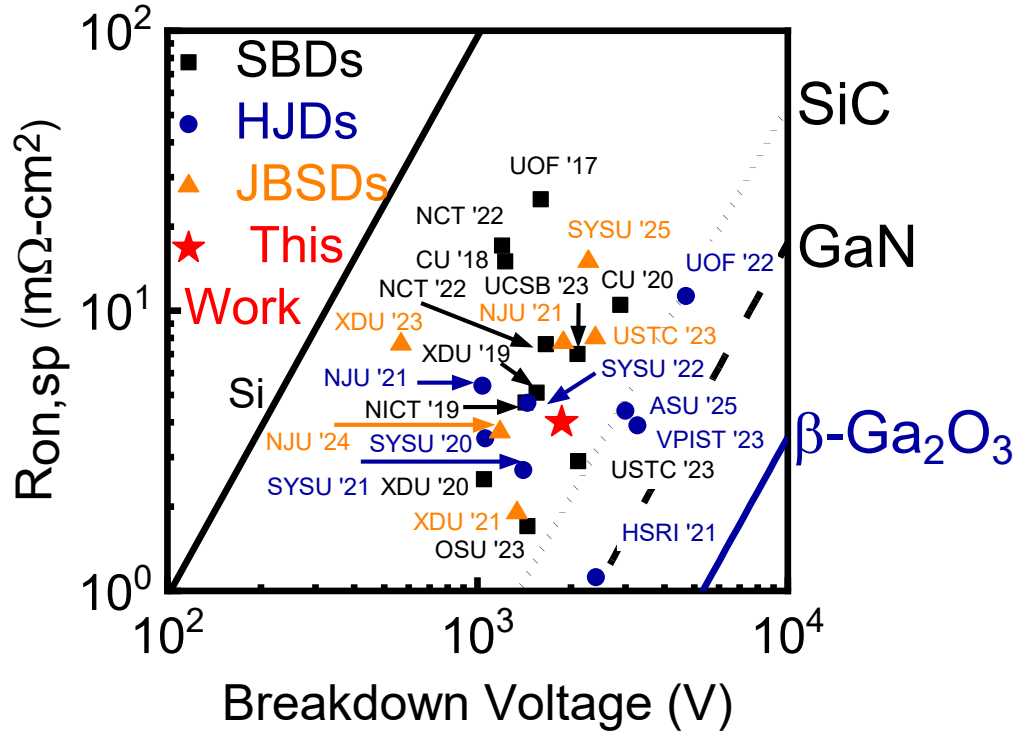


FIG. 8. Benchmarking of our best device with state-of-the-art Ga_2O_3 vertical SBDs, HJDs, and JBSDs.

The benchmark comparison of our trench JBSDs with prior reports of SBDs, HJDs, and JBSDs in terms of on-state resistance and breakdown voltage is shown in Fig. 8. The best performing JBSDs ($W_f=0.85\mu\text{m}$) shows a power figure of merit of 0.7 GW-cm^{-2} ($V_B \sim 1867\text{V}$ and $R_{\text{on,sp}} \sim 4\text{m}\Omega\text{-cm}^2$) which is comparable to previous reports of vertical Ga_2O_3 diodes.^{24,25,27–46}

IV. CONCLUSION

In conclusion, we demonstrated trench junction barrier Schottky diodes integrated with Space Modulated-Junction termination extension achieving kV-class reverse breakdown performance and low turn on voltage close to 1 V. An effective tri-layer mask

process with Ni/SiN_x/SiO₂ was used to etch the trenches and for deposition and lift-off of NiO from the top-side of the trenches. The reverse breakdown for the best performing diodes was around 2kV which resulted in unipolar PFOM of $\sim 0.7 \text{ GW-cm}^{-2}$. These results exhibit the great potential of NiO/Ga₂O₃ junction barrier schottky diodes for low loss kilovolt class power electronics applications.

ACKNOWLEDGMENTS

This work was supported by NSF ECCS-2336397 and in part by ULTRA, an EFRC center by DOE, Office of Science, Basic Energy Sciences under award No DE-SC0021230. The work in ASU NanoFab was supported in part by the National Science Foundation award ECCS-2025490. We acknowledge the use of facilities within the Eyring Materials Center at Arizona State University supported in part by NNCI-ECCS-1542160.

REFERENCES

- ¹ J.Y. Tsao, S. Chowdhury, M.A. Hollis, D. Jena, N.M. Johnson, K.A. Jones, R.J. Kaplar, S. Rajan, C.G. Van De Walle, E. Bellotti, C.L. Chua, R. Collazo, M.E. Coltrin, J.A. Cooper, K.R. Evans, S. Graham, T.A. Grotjohn, E.R. Heller, M. Higashiwaki, M.S. Islam, P.W. Juodawlkis, M.A. Khan, A.D. Koehler, J.H. Leach, U.K. Mishra, R.J. Nemanich, R.C.N. Pilawa-Podgurski, J.B. Shealy, Z. Sitar, M.J. Tadjer, A.F. Witulski, M. Wraback, and J.A. Simmons, "Ultrawide-Bandgap Semiconductors: Research Opportunities and Challenges," *Adv. Electron. Mater.* **4**(1), 1600501 (2018).
- ² K.D. Chabak, K.D. Leedy, A.J. Green, S. Mou, A.T. Neal, T. Asel, E.R. Heller, N.S. Hendricks, K. Liddy, A. Crespo, N.C. Miller, M.T. Lindquist, N.A. Moser, R.C. Fitch, D.E. Walker, D.L. Dorsey, and G.H. Jessen, "Lateral β -Ga₂O₃ field effect transistors," *Semicond. Sci. Technol.* **35**(1), 013002 (2020).
- ³ M.J. Tadjer, "Toward gallium oxide power electronics," *Science* **378**(6621), 724–725 (2022).
- ⁴ A.J. Green, J. Speck, G. Xing, P. Moens, F. Allerstam, K. Gumaelius, T. Neyer, A. Arias-Purdue, V. Mehrotra, A. Kuramata, K. Sasaki, S. Watanabe, K. Koshi, J. Blevins, O. Bierwagan, S. Krishnamoorthy, K. Leedy, A.R. Arehart, A.T. Neal, S. Mou, S.A. Ringel, A.

- Kumar, A. Sharma, K. Ghosh, U. Singiseti, W. Li, K. Chabak, K. Liddy, A. Islam, S. Rajan, S. Graham, S. Choi, Z. Cheng, and M. Higashiwaki, “ β -Gallium oxide power electronics,” *APL Materials* **10**(2), 029201 (2022).
- ⁵ M. Higashiwaki, “ β -Gallium Oxide Devices: Progress and Outlook,” *Phys. Status Solidi RRL* **15**(11), 2100357 (2021).
- ⁶ M. Higashiwaki, and G.H. Jessen, “Guest Editorial: The dawn of gallium oxide microelectronics,” *Applied Physics Letters* **112**(6), 060401 (2018).
- ⁷ B.R. Tak, S. Kumar, A.K. Kapoor, D. Wang, X. Li, H. Sun, and R. Singh, “Recent advances in the growth of gallium oxide thin films employing various growth techniques—a review,” *J. Phys. D: Appl. Phys.* **54**(45), 453002 (2021).
- ⁸ L. Huang, H. Tang, C. Zhang, P. Sun, Q. Fang, F. Wu, P. Luo, B. Liu, and J. Xu, “Growth of gallium oxide bulk crystals: a review,” *Eur. Phys. J. Spec. Top.* **234**(2), 231–271 (2025).
- ⁹ J. Zhang, P. Dong, K. Dang, Y. Zhang, Q. Yan, H. Xiang, J. Su, Z. Liu, M. Si, J. Gao, M. Kong, H. Zhou, and Y. Hao, “Ultra-wide bandgap semiconductor Ga₂O₃ power diodes,” *Nat Commun* **13**(1), 3900 (2022).
- ¹⁰ S. Roy, B. Kostroun, J. Cooke, Y. Liu, A. Bhattacharyya, C. Peterson, B. Sensale-Rodriguez, and S. Krishnamoorthy, “Ultra-low reverse leakage in large area kilo-volt class β -Ga₂O₃ trench Schottky barrier diode with high-k dielectric RESURF,” *Applied Physics Letters* **123**(24), (2023).
- ¹¹ Z. Liu, P.-G. Li, Y.-S. Zhi, X.-L. Wang, X.-L. Chu, and W.-H. Tang, “Review of gallium oxide based field-effect transistors and Schottky barrier diodes,” *Chinese Phys. B* **28**(1), 017105 (2019).
- ¹² M.H. Wong, and M. Higashiwaki, “Vertical β -Ga₂O₃ Power Transistors: A Review,” *IEEE Trans. Electron Devices* **67**(10), 3925–3937 (2020).
- ¹³ A. Gilankar, A. Katta, N. Das, and N.K. Kalarickal, “>3kV NiO/Ga₂O₃ Heterojunction Diodes With Space-Modulated Junction Termination Extension and Sub-1V Turn-On,” *IEEE J. Electron Devices Soc.* **13**, 373–377 (2025).
- ¹⁴ M. Xiao, B. Wang, J. Spencer, Y. Qin, M. Porter, Y. Ma, Y. Wang, K. Sasaki, M. Tadjer, and Y. Zhang, “NiO junction termination extension for high-voltage (> 3 kV) Ga₂O₃ devices,” *Applied Physics Letters* **122**(18), 183501 (2023).
- ¹⁵ H. Gong, Z. Wang, X. Yu, F. Ren, Y. Yang, Y. Lv, Z. Feng, S. Gu, R. Zhang, Y. Zheng, and J. Ye, “Field-Plated NiO/Ga₂O₃ p-n Heterojunction Power Diodes With High-Temperature Thermal Stability and Near Unity Ideality Factors,” *IEEE J. Electron Devices Soc.* **9**, 1166–1171 (2021).
- ¹⁶ W. Hao, Q. He, X. Zhou, X. Zhao, G. Xu, and S. Long, “2.6 kV NiO/Ga₂O₃ Heterojunction Diode with Superior High-Temperature Voltage Blocking Capability,” in *2022 IEEE 34th International Symposium on Power Semiconductor Devices and ICs (ISPSD)*, (IEEE, Vancouver, BC, Canada, 2022), pp. 105–108.
- ¹⁷ Y. Wang, H. Gong, Y. Lv, X. Fu, S. Dun, T. Han, H. Liu, X. Zhou, S. Liang, J. Ye, R. Zhang, A. Bu, S. Cai, and Z. Feng, “2.41 kV Vertical P-NiO/n-Ga₂O₃ Heterojunction Diodes With a Record Baliga’s Figure-of-Merit of 5.18 GW/cm²,” *IEEE Trans. Power Electron.* **37**(4), 3743–3746 (2022).
- ¹⁸ Y. Liu, S. Roy, C. Peterson, A. Bhattacharyya, and S. Krishnamoorthy, “Ultra-low reverse leakage NiOx/ β -Ga₂O₃ heterojunction diode achieving breakdown voltage >3 kV with plasma etch field-termination,” *AIP Advances* **15**(1), (2025).
- ¹⁹ D. Liu, Z. Zhang, H. Chen, X. Tian, Y. Wang, Y. Yan, L. Zeng, X. Liu, D. Chen, Q. Feng, H. Zhou, Z. Liu, J. Zhang, C. Zhang, and Y. Hao, “Performance Enhancement of NiO_x/ β -Ga₂O₃ Heterojunction Diodes by Synergistic Interface Engineering,” *IEEE Trans. Electron Devices* **71**(8), 4578–4583 (2024).

- ²⁰ J. Wan, H. Wang, C. Zhang, Y. Li, C. Wang, H. Cheng, J. Li, N. Ren, Q. Guo, and K. Sheng, “3.3 kV-class NiO/ β -Ga₂O₃ heterojunction diode and its off-state leakage mechanism,” *Applied Physics Letters* **124**(24), (2024).
- ²¹ X. Lu, Y. Deng, Y. Pei, Z. Chen, and G. Wang, “Recent advances in NiO/Ga₂O₃ heterojunctions for power electronics,” *J. Semicond.* **44**(6), 061802 (2023).
- ²² J.-S. Li, C.-C. Chiang, X. Xia, T.J. Yoo, F. Ren, H. Kim, and S.J. Pearton, “Demonstration of 4.7 kV breakdown voltage in NiO/ β -Ga₂O₃ vertical rectifiers,” *Applied Physics Letters* **121**(4), 042105 (2022).
- ²³ X. Lu, X. Zhou, H. Jiang, K.W. Ng, Z. Chen, Y. Pei, K.M. Lau, and G. Wang, “1-kV Sputtered p-NiO/n-Ga₂O₃ Heterojunction Diodes With an Ultra-Low Leakage Current Below $1\text{ }\mu\text{A}/\text{cm}^2$,” *IEEE Electron Device Lett.* **41**(3), 449–452 (2020).
- ²⁴ H. Gong, N. Sun, T. Hu, X. Yu, M. Porter, Z. Yang, F. Ren, S. Gu, Y. Zheng, R. Zhang, Y. Zhang, and J. Ye, “Ga₂O₃/NiO junction barrier Schottky diodes with ultra-low barrier TiN contact,” *Applied Physics Letters* **124**(23), (2024).
- ²⁵ H.H. Gong, X.X. Yu, Y. Xu, X.H. Chen, Y. Kuang, Y.J. Lv, Y. Yang, F.-F. Ren, Z.H. Feng, S.L. Gu, Y.D. Zheng, R. Zhang, and J.D. Ye, “ β -Ga₂O₃ vertical heterojunction barrier Schottky diodes terminated with p-NiO field limiting rings,” *Applied Physics Letters* **118**(20), (2021).
- ²⁶ H. Zhou, S. Zeng, J. Zhang, Z. Liu, Q. Feng, S. Xu, J. Zhang, and Y. Hao, “Comprehensive Study and Optimization of Implementing p-NiO in β -Ga₂O₃ Based Diodes via TCAD Simulation,” *Crystals* **11**(10), 1186 (2021).
- ²⁷ S. Roy, *2.1 kV (001)- β -Ga₂O₃ Vertical Schottky Barrier Diode with High-k Oxide Field Plate* (2022).
- ²⁸ W. Li, K. Nomoto, Z. Hu, D. Jena, and H.G. Xing, “Field-Plated Ga₂O₃ Trench Schottky Barrier Diodes With a $\text{BV}^2/\text{R}_{\text{on,sp}}$ of up to 0.95 GW/cm²,” *IEEE Electron Device Lett.* **41**(1), 107–110 (2020).
- ²⁹ W. Li, Z. Hu, K. Nomoto, Z. Zhang, J.-Y. Hsu, Q.T. Thieu, K. Sasaki, A. Kuramata, D. Jena, and H.G. Xing, “1230 V β -Ga₂O₃ trench Schottky barrier diodes with an ultra-low leakage current of $<1\text{ }\mu\text{A}/\text{cm}^2$,” *Applied Physics Letters* **113**(20), 202101 (2018).
- ³⁰ S. Dhara, N.K. Kalarickal, A. Dheenan, S.I. Rahman, C. Joishi, and S. Rajan, “ β -Ga₂O₃ trench Schottky diodes by low-damage Ga-atomic beam etching,” *Applied Physics Letters* **123**(2), 023503 (2023).
- ³¹ C. Liao, X. Lu, T. Xu, P. Fang, Y. Deng, H. Luo, Z. Wu, Z. Chen, J. Liang, Y. Pei, and G. Wang, “Optimization of NiO/ β -Ga₂O₃ Heterojunction Diodes for High-Power Application,” *IEEE Trans. Electron Devices* **69**(10), 5722–5727 (2022).
- ³² S. Roy, A. Bhattacharyya, P. Ranga, H. Splawn, J. Leach, and S. Krishnamoorthy, “High-k Oxide Field-Plated Vertical (001) β -Ga₂O₃ Schottky Barrier Diode With Baliga’s Figure of Merit Over 1 GW/cm²,” *IEEE Electron Device Lett.* **42**(8), 1140–1143 (2021).
- ³³ H. Luo, X. Zhou, Z. Chen, Y. Pei, X. Lu, and G. Wang, “Fabrication and Characterization of High-Voltage NiO/ β -Ga₂O₃ Heterojunction Power Diodes,” *IEEE Trans. Electron Devices* **68**(8), 3991–3996 (2021).
- ³⁴ S. Kumar, H. Murakami, Y. Kumagai, and M. Higashiwaki, “Vertical β -Ga₂O₃ Schottky barrier diodes with trench staircase field plate,” *Appl. Phys. Express* **15**(5), 054001 (2022).
- ³⁵ Z. Hu, Y. Lv, C. Zhao, Q. Feng, Z. Feng, K. Dang, X. Tian, Y. Zhang, J. Ning, H. Zhou, X. Kang, J. Zhang, and Y. Hao, “Beveled Fluoride Plasma Treatment for Vertical β -Ga₂O₃ Schottky Barrier Diode With High Reverse Blocking Voltage and Low Turn-On Voltage,” *IEEE Electron Device Lett.* **41**(3), 441–444 (2020).

- ³⁶ J. Yang, S. Ahn, F. Ren, S.J. Pearton, S. Jang, and A. Kuramata, “High Breakdown Voltage (~ 201 V) β -Ga₂O₃ Schottky Rectifiers,” IEEE Electron Device Lett. **38**(7), 906–909 (2017).
- ³⁷ F. Otsuka, H. Miyamoto, A. Takatsuka, S. Kunori, K. Sasaki, and A. Kuramata, “Large-size (1.7×1.7 mm²) β -Ga₂O₃ field-plated trench MOS-type Schottky barrier diodes with 1.2 kV breakdown voltage and 10^9 high on/off current ratio,” Appl. Phys. Express **15**(1), 016501 (2022).
- ³⁸ C. Wang, H. Gong, W. Lei, Y. Cai, Z. Hu, S. Xu, Z. Liu, Q. Feng, H. Zhou, J. Ye, J. Zhang, R. Zhang, and Y. Hao, “Demonstration of the p-NiO_x/n-Ga₂O₃ Heterojunction Gate FETs and Diodes With BV²/R_{on,sp} Figures of Merit of 0.39 GW/cm² and 1.38 GW/cm²,” IEEE Electron Device Lett. **42**(4), 485–488 (2021).
- ³⁹ J.-S. Li, H.-H. Wan, C.-C. Chiang, T.J. Yoo, F. Ren, H. Kim, and S.J. Pearton, “NiO/Ga₂O₃ Vertical Rectifiers of 7 kV and 1 mm² with 5.5 A Forward Conduction Current,” Crystals **13**(12), 1624 (2023).
- ⁴⁰ H. Zhou, Q. Feng, J. Ning, C. Zhang, P. Ma, Y. Hao, Q. Yan, J. Zhang, Y. Lv, Z. Liu, Y. Zhang, K. Dang, P. Dong, and Z. Feng, “High-Performance Vertical β -Ga₂O₃ Schottky Barrier Diode With Implanted Edge Termination,” IEEE Electron Device Lett. **40**(11), 1788–1791 (2019).
- ⁴¹ W. Hao, F. Wu, W. Li, G. Xu, X. Xie, K. Zhou, W. Guo, X. Zhou, Q. He, X. Zhao, S. Yang, and S. Long, “Improved Vertical β -Ga₂O₃ Schottky Barrier Diodes With Conductivity-Modulated p-NiO Junction Termination Extension,” IEEE Trans. Electron Devices **70**(4), 2129–2134 (2023).
- ⁴² A.E. Islam, C. Zhang, K. DeLello, D.A. Muller, K.D. Leedy, S. Ganguli, N.A. Moser, R. Kahler, J.C. Williams, D.M. Dryden, S. Tetlak, K.J. Liddy, A.J. Green, and K.D. Chabak, “Defect Engineering at the Al₂O₃/(010) β -Ga₂O₃ Interface via Surface Treatments and Forming Gas Post-Deposition Anneals,” IEEE Trans. Electron Devices **69**(10), 5656–5663 (2022).
- ⁴³ S. Cheng, Y. Lai, X. Lu, T. Luo, H. Luo, H. Hu, R. Zhou, H. Jiang, Z. Wu, J. Liang, Z. Chen, G. Wang, and Y. Pei, “Low Leakage Current β -Ga₂O₃ Self-Aligned Trench Junction Barrier Schottky Diodes,” IEEE Trans. Electron Devices **72**(7), 3497–3501 (2025).
- ⁴⁴ F. Zhang, X. Zheng, Y. He, X. Wang, Y. Hong, X. Zhang, Z. Yuan, Y. Wang, X. Lu, J. Yin, Y. Gao, X. Ma, and Y. Hao, “The Impact of Anode p⁺ Islands Layout on the Performance of NiO_x/ β -Ga₂O₃ Hetero-Junction Barrier Schottky Diodes,” IEEE Trans. Electron Devices **70**(11), 5603–5608 (2023).
- ⁴⁵ Q. Yan, H. Gong, J. Zhang, J. Ye, H. Zhou, Z. Liu, S. Xu, C. Wang, Z. Hu, Q. Feng, J. Ning, C. Zhang, P. Ma, R. Zhang, and Y. Hao, “ β -Ga₂O₃ hetero-junction barrier Schottky diode with reverse leakage current modulation and BV²/R_{on,sp} value of 0.93 GW/cm²,” Applied Physics Letters **118**(12), 122102 (2021).
- ⁴⁶ F. Wu, Y. Wang, G. Jian, G. Xu, X. Zhou, W. Guo, J. Du, Q. Liu, S. Dun, Z. Yu, Y. Lv, Z. Feng, S. Cai, and S. Long, “Superior Performance β -Ga₂O₃ Junction Barrier Schottky Diodes Implementing p-NiO Heterojunction and Beveled Field Plate for Hybrid Cockcroft–Walton Voltage Multiplier,” IEEE Trans. Electron Devices **70**(3), 1199–1205 (2023).